Supplemental Figures.

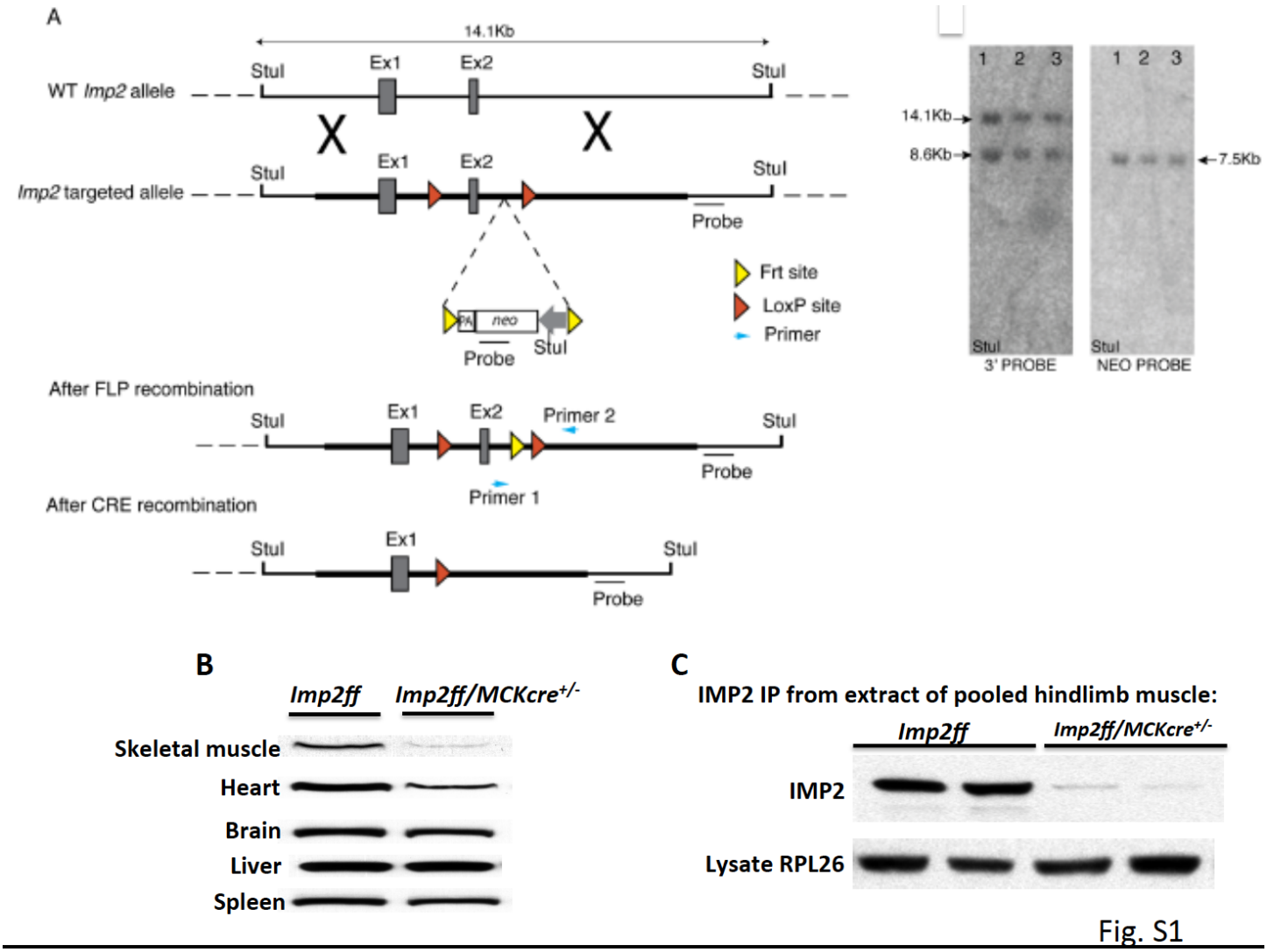

Figure S1. Generation of a floxed *Imp2* allele, and analysis of IMP2 abundance in tissues from *Imp2ff* and *Imp2ff/MCK-cre*$^{+/-}$ mice. Refers to Figure 1.

A. Schematic representation of the *Imp2* wt and targeted allele showing exon 1-2 and flanking intron sequences. The Imp2 targeted allele was assembled by ET recombineering. A LoxP site (red triangle) was inserted upstream of exon2 (Ex2), followed by the insertion of Frt sequences (yellow triangle) flanked neo cassette (for Flp-mediated removal in vivo) into the intron 2/3 of the Imp2 gene, followed by a second Lox P site. The position of the 3' and neo probes, the StuI enzyme restriction site used for the southern analysis, as well as the position of the primers (1, 2) used for the PCR strategy are indicated. The schematic view of successful neo deletion after Flp recombination and successful deletion of *Imp2* exon 2 after Cre recombination are also indicated. Southern blot analysis (right) showing 3 correctly targeted ES clones, using a 3' probe (PCR fragment of 527 bp) downstream of exon 2 and a Neo probe (PCR fragment of 700 bp). DNA was digested with StuI enzyme and 3' prime as well as Neo probes were used in this analysis.

B. Immunoblot of IMP2 in selected tissues of *Imp2ff* and and *Imp2ff/MCK-cre*$^{+/-}$ mice.

C. Immunoblot of IMP2 immunoprecipitated from skeletal muscle of *Imp2ff* and *Imp2ff/MCK-cre*$^{+/-}$ mice.

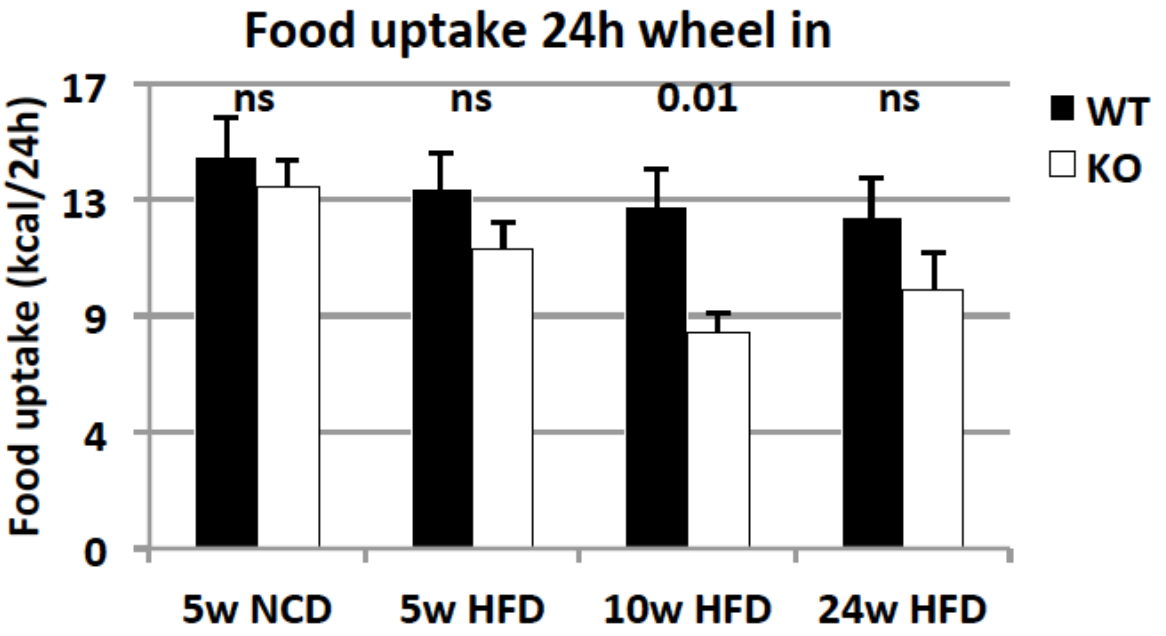

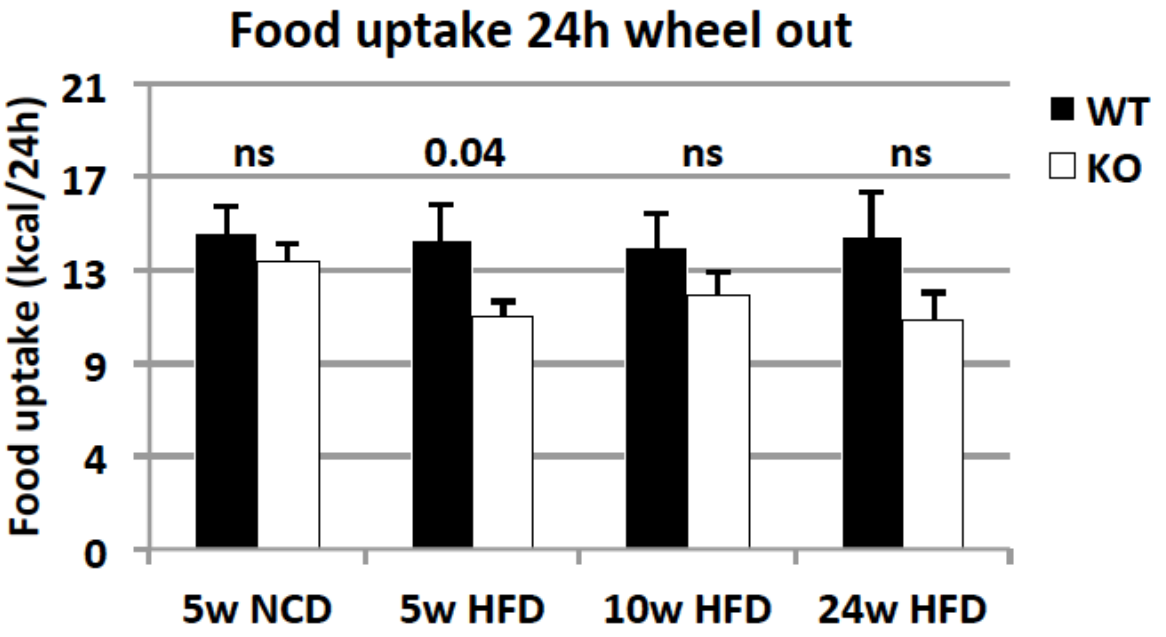

Fig. S2

Figure S2. Food intake of *Imp2ff* and *Imp2ff/MCK-cre*$^{+/-}$ mice at several ages. Refers to Fig. 3
Upper-during access to running wheel.
Lower-intake with wheel blocked.

GSEA of proteome: Imp2ff/Imp2ff/MCKcre

Gene set	Size	ES	NES	NOM p-val	FDR q-val	FWER p-val
Hallmark Oxidative Phosphorylation	157	0.42	1.81	0.000	0.040	0.034

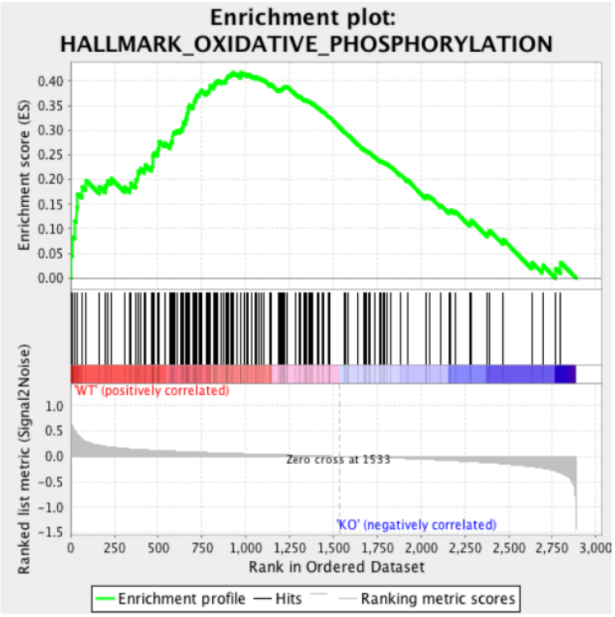

Fig. S3

Figure S3. Analysis of muscle proteome by Gene set enrichment analysis shows that proteins involved in oxidative phosphorylation are enriched in Imp2ff muscle as compared with *Imp2ff/MCK-cre*$^{+/-}$ muscle. Refers to Figures 4 and 5.

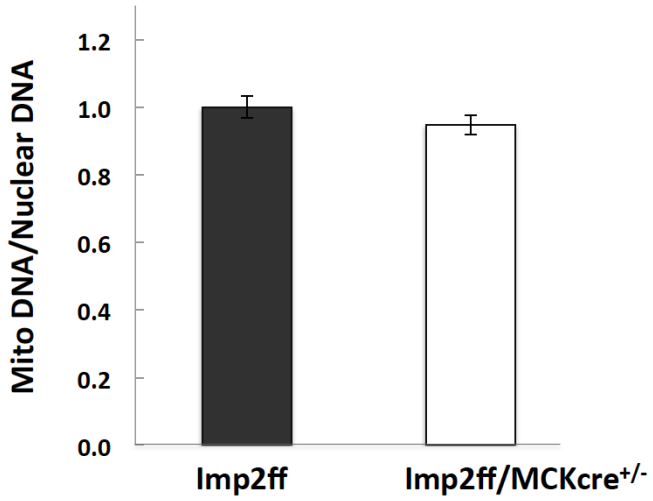

Fig. S4

Figure S4. The ratio of mitochondrial DNA to nuclear DNA in *Imp2ff* and *Imp2ff/MCK-cre*$^{+/-}$ Skeletal muscle. Refers to Fig. 4. Estimated by QPCR from soleus, N=6 pairs.

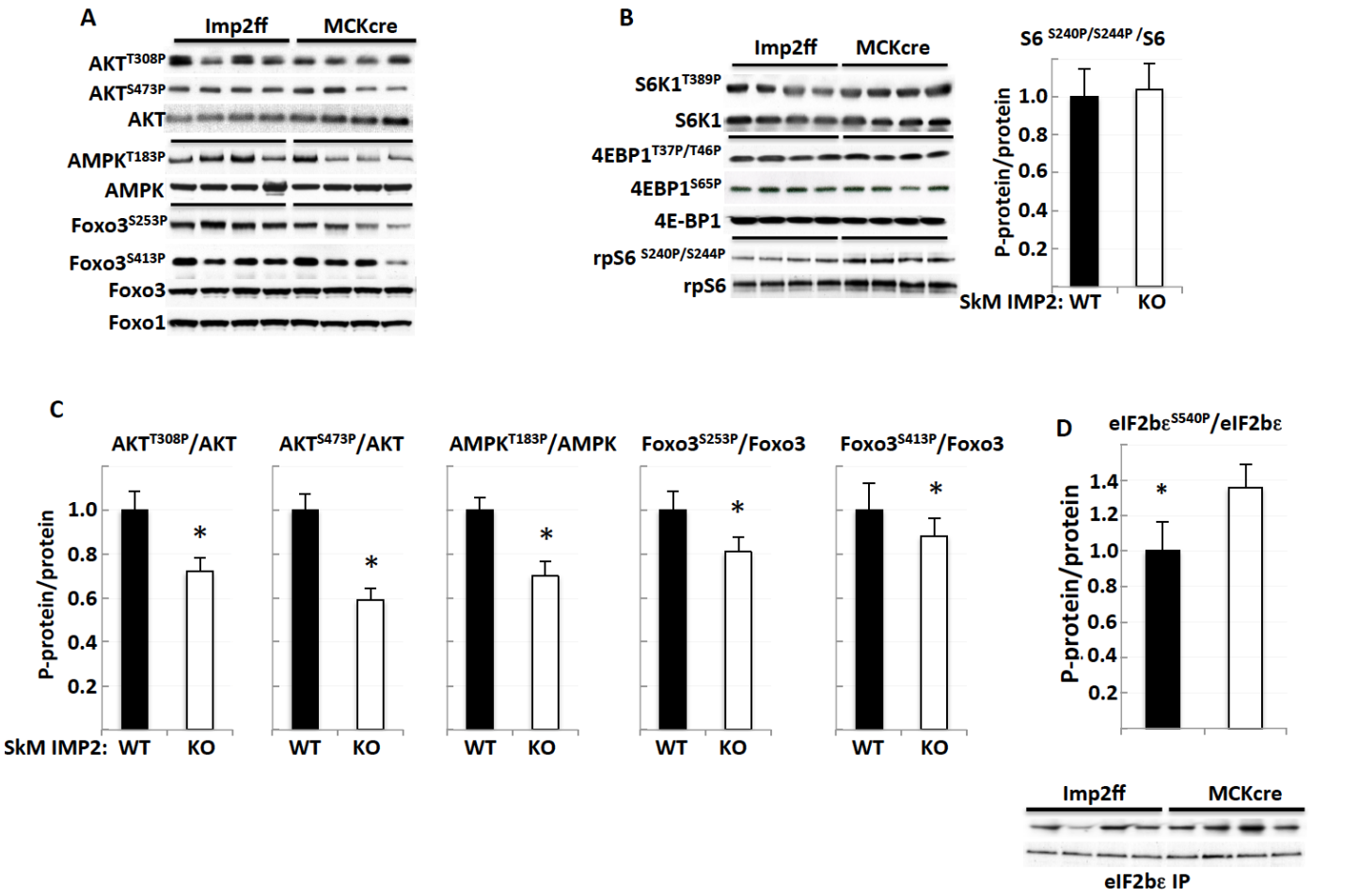

Fig. S5

Figure S5. Abundance and phosphorylation state of Akt1+2, AMPK and Foxo3. Refers to Figure 7.
A. Immunoblots of total Akt and Akt(T308P) and (S473P), AMPK and AMPK(T183P), Foxo 1, Foxo3, Foxo3(S253P) and (S413P) in skeletal muscle from *Imp2ff* amd *Imp2ff/MCK-cre*$^{+/-}$ mice. Phosphorylation at AktT308 and S473, and at AMPKT183 are activating; phosphorylation at Foxo3(S253) (by Akt) is inhibitory whereas phosphorylation at Foxo3(S413) (by AMPK) is activating.
B. The phosphorylation state of S6K1[Thr389], 4EBP1[Thr37/46,Ser65] and rpS6[Ser240/244] in *Imp2ff* and *Impff/MCKcre*$^{+/-}$ muscle. Quantitation of S6K1 and 4EBP1 is shown in Fig. 7C.
C. Quantitation of the Phospho-specific immunoblots in A. * = $p<0.05$.
D. eIF2Bε was IPed from extracts of *Imp2 ff* and *Imp2ff/MCK-cre*$^{+/-}$ skeletal muscle and immunoblotted for eIF2Bε polypeptide and eIF2Bε(S540P). * = $p<0.05$.